Behavioral/Cognitive

Maladaptive Laterality in Cortical Networks Related to Social Communication in Autism Spectrum Disorder

Andrew S. Persichetti, Jiayu Shao, Stephen J. Gotts, and Alex Martin

Section on Cognitive Neuropsychology, Laboratory of Brain and Cognition, National Institute of Mental Health, National Institutes of Health, Bethesda, Maryland 20892

Neuroimaging studies of individuals with autism spectrum disorders (ASDs) consistently find an aberrant pattern of reduced laterality in brain networks that support functions related to social communication and language. However, it is unclear how the underlying functional organization of these brain networks is altered in ASD individuals. We tested four models of reduced laterality in a social communication network in 70 ASD individuals (14 females) and a control group of the same number of tightly matched typically developing (TD) individuals (19 females) using high-quality resting-state fMRI data and a method of measuring patterns of functional laterality across the brain. We found that a functionally defined social communication network exhibited the typical pattern of left laterality in both groups, whereas there was a significant increase in within- relative to across-hemisphere connectivity of homotopic regions in the right hemisphere in ASD individuals. Furthermore, greater within- relative to across-hemisphere connectivity in the left hemisphere was positively correlated with a measure of verbal ability in both groups, whereas greater within- relative to across-hemisphere connectivity in the right hemisphere in ASD, but not TD, individuals was negatively correlated with the same verbal measure. Crucially, these differences in patterns of laterality were not found in two other functional networks and were specifically correlated to a measure of verbal ability but not metrics of other core components of the ASD phenotype. These results suggest that previous reports of reduced laterality in social communication regions in ASD is because of the two hemispheres functioning more independently than seen in TD individuals, with the atypical right-hemisphere network component being maladaptive.

Key words: autism spectrum disorder; laterality; resting-state fMRI; social communication

---

Significance Statement

A consistent neuroimaging finding in individuals with ASD is an aberrant pattern of reduced laterality of the brain networks that support functions related to social communication and language. We tested four models of reduced laterality in a social communication network in ASD individuals and a TD control group using high-quality resting-state fMRI data. Our results suggest that reduced laterality of social communication regions in ASD may be because of the two hemispheres functioning more independently than seen in TD individuals, with atypically greater within- than across-hemisphere connectivity in the right hemisphere being maladaptive.

Introduction

Impaired social communication is a core behavioral phenotype across the autism spectrum, ranging from a complete lack of ability on the low end to subtle deficits in high-functioning individuals (Goldstein et al., 1994; Boucher, 2003, 2012; Rapin and Dunn, 2003; American Psychiatric Association, 2013). Consistent with

these behavioral deficits, one of the most robust neuroimaging findings in (usually high functioning) individuals with autism spectrum disorders (ASDs) is an aberrant pattern of reduced laterality of the brain networks that support functions related to social communication and language (Lindell and Hudry, 2013; Herringshaw et al., 2016). For example, functional MRI (fMRI) studies that use communication- and language-based tasks consistently find a reduced difference in the magnitude of neural responses between typically left-lateralized regions and homotopic regions in the right hemisphere in ASD compared with typically developing (TD) individuals (Herbert et al., 2002; Boddaert et al., 2003; Takeuchi et al., 2004; Harris et al., 2006; Wang et al., 2006; Kleinhans et al., 2008; Knaus et al., 2008, 2010; Redcay and Courchesne, 2008; Tesink et al., 2009; Anderson et al., 2010; Eyler et al., 2012; Jouravlev et al., 2020). Although such results suggest that typically left-lateralized cortical networks that

support social communication and language are more symmetrically distributed across hemispheres in ASD, hemispheric differences in task-based responses between ASD and TD groups could be because of several underlying changes to the functional organization of these brain networks. For example, atypical patterns of task responses in ASD could be because of an intact left-lateralized cortical network communicating more with the right hemisphere or a weakened left-lateralized network that results in compensatory activity in the right hemisphere. Therefore, it is necessary to measure patterns of functional connectivity within and across hemispheres to understand how brain networks underlying social communication are reorganized in ASD.

In TD individuals, left-lateralized networks that support functions requiring rapid cortical interactions, such as language, communication, and fine motor control, tend to communicate more exclusively within hemisphere than with regions in the right hemisphere (Semmes, 1968; Lackner and Teuber, 1973; Poeppel, 2003). In contrast, typically right-lateralized networks that support functions requiring integration of information across the hemispheres (e.g., the right-lateralized visuospatial attention network requires bilateral representations of space) also communicate strongly with left hemisphere regions (Corbetta and Shulman, 2011). To probe these distinct patterns of lateralization, a previous study developed two metrics of laterality based on patterns of resting-state functional connectivity, one that measures the tendency for greater within-hemisphere than across-hemisphere communication from the left versus the right hemisphere, referred to as Segregation, and another that measures a greater sum of within- and across-hemisphere communication from the left versus the right hemisphere, referred to as Integration. The authors found that the degree to which regions in a left-segregated frontotemporal network were left lateralized was positively correlated with a measure of verbal ability, whereas the degree to which regions in the right-lateralized visuospatial attention network were integrated with the left hemisphere was positively correlated with visuospatial ability (Gotts et al., 2013). In the current study, we use these validated laterality metrics to adjudicate between potential models of reduced left laterality in social communication regions in ASD.

Materials and Methods

Participants. After excluding participants from each group based on data quality metrics (see below), we analyzed the data from 70 individuals [mean (SD) age = 19 (3.8) years, 14 female] who met the *Diagnostic and Statistical Manual of Mental Disorders: DSM-5* criteria for ASD (American Psychiatric Association, 2013) as assessed by a trained clinician and 70 individuals with not a history of psychiatric or neurologic disorders [mean (SD) age = 19.7 (3.7) years, 19 female], which served as the TD control group. There was not a significant difference between the ages of the two groups ($t_{(138)} = 1.14$, $p = 0.26$, $d = 0.19$). Subsets of the resting-state data from these individuals have been used in a number of our previous studies (Gotts et al., 2012, 2013; Ramot et al., 2017; Jasmin et al., 2019; Power et al., 2019; Persichetti et al., 2021). All participants gave informed consent under a protocol approved by the National Institutes of Health Institutional Review Board (10 M-0027, clinical trials number NCT01031407).

Behavioral measures. The Wechsler Abbreviated Scale of Intelligence (WASI; Wechsler, 1999) was administered within 1 year of the scanning session to all participants in each group [mean (SD) full-score IQ, TD, 116.1 (11); ASD, 114.2 (12.9); $t_{(138)} = 1.15$, $p = 0.25$, $d = 0.16$]. We used the individual T scores (normative mean = 50, SD = 10) from the Vocabulary and Block Design subtests of the WASI in a correlation analysis with the neuroimaging data. These scores were missing from one participant in each group. We chose the Vocabulary and Block Design subtests because they have been shown to have strong and selective associations with verbal/language and visuospatial abilities, respectively

(Warrington et al., 1986; Gotts et al., 2013; Kenworthy et al., 2013). We also obtained scores on two quantitative informant-based rating scales that measure symptoms over the full range of severity as indicated by the parents of ASD participants. The Social Responsiveness Scale (Constantino et al., 2003) was used to assess social traits, and the Repetitive Behaviors Scale–Revised (Lam and Aman, 2007) was used to assess restricted repetitive behaviors.

MRI data acquisition. Scanning was completed on a Signa HDxt 3.0 T scanner (GE Healthcare) at the National Institutes of Health Clinical Center Nuclear Magnetic Resonance Research Facility. For each participant, T2*-weighted blood oxygen level-dependent (BOLD) images covering the whole brain were acquired using an eight-channel receive-only head coil and a gradient echo single-shot echoplanar imaging sequence [repetition time (TR) = 3500 ms, echo time = 27 ms, flip angle = 90°, 42 axial contiguous interleaved slices per volume, 3.0 mm slice thickness, field of view (FOV) = 22 cm, 128 × 128 acquisition matrix, single-voxel volume $1.7 × 1.7 × 3.0 \, mm^3$]. An acceleration factor of 2 (Array Spatial Sensitivity Encoding Technique) was used to reduce gradient coil heating during the session. In addition to the functional images, a high-resolution T1-weighted anatomic image [magnetization-prepared rapid acquisition with gradient echo (MPRAGE)] was obtained (124 axial slices, 1.2 mm slice thickness, FOV = 24 cm, 224 × 224 acquisition matrix).

fMRI procedure. During the resting scans, participants were instructed to relax and keep their eyes fixated on a central cross. Each resting scan lasted 8 min 10 s for a total of 140 consecutive whole-brain volumes. Independent measures of cardiac and respiratory cycles were recorded during scanning for later artifact removal.

fMRI data preprocessing. All data were preprocessed using the Analysis of Functional Neuro Images (AFNI) software package (Cox, 1996). First, the initial three TRs from each EPI scan were removed to allow for T1 equilibration. Next, 3dDespike was used to bound outlying time points in each voxel within 4 SDs of the time series mean, and 3dTshift was used to adjust for slice acquisition time within each volume (to $t = 0$). Then 3dvolreg was used to align each volume of the resting-state scan series to the first retained volume of the scan. White matter and large ventricle masks were created from the aligned MPRAGE scan using FreeSurfer software (Fischl et al., 2002). These masks were then resampled to EPI resolution, eroded by one voxel to prevent partial volume effects with gray matter voxels, and applied to the volume-registered data to generate white matter and ventricle nuisance regressors before spatial blurring. Scans were then spatially blurred by a 6 mm Gaussian kernel (full-width at half-maximum) and divided by the mean of the voxelwise time series to yield units of percentage signal change.

The data were denoised using the ANATICOR preprocessing approach (Jo et al., 2010). Nuisance regressors for each voxel included six head-position parameter time series (three translation, three rotation); one average eroded ventricle time series; one localized eroded white matter time series (averaging the time series of all white matter voxels within a 15-mm-radius sphere); eight RETROICOR time series (four cardiac, four respiration), calculated from the cardiac and respiratory measures taken during the scan (Glover et al., 2000); and five respiration volume per time time series to minimize end-tidal CO_2 effects from deep breaths (Birn et al., 2008). All regressors were detrended with a fourth-order polynomial before denoising, and the same detrending was applied during nuisance regression to the voxel time series. Finally, the residual time series were spatially transformed to standard anatomic space (Talairach–Tournoux).

To ensure that the fMRI data from both groups were high quality and matched, we measured the temporal signal-to-noise-ratio (tSNR) across the whole brain and a summary of in-scanner head motion using the @1dDiffMag program in AFNI. We calculated the tSNR in each voxel as the time series mean divided by time series SD. We used DiffMag (comparable to mean framewise displacement, Power et al., 2012), which estimates the average of first differences in frame-to-frame motion across each scan run, to exclude participants with scores >0.2 mm/TR. We then selected participants from both groups that had the highest tSNR values and lowest in-scanner head motion while ensuring that both quality metrics were matched between the groups (tSNR, $t_{(138)} = 0.61$, $p = 0.54$, d = 0.10; DiffMag, $t_{(138)} = 1.54$, $p = 0.13$, d = 0.26; Fig. 1).

A

B
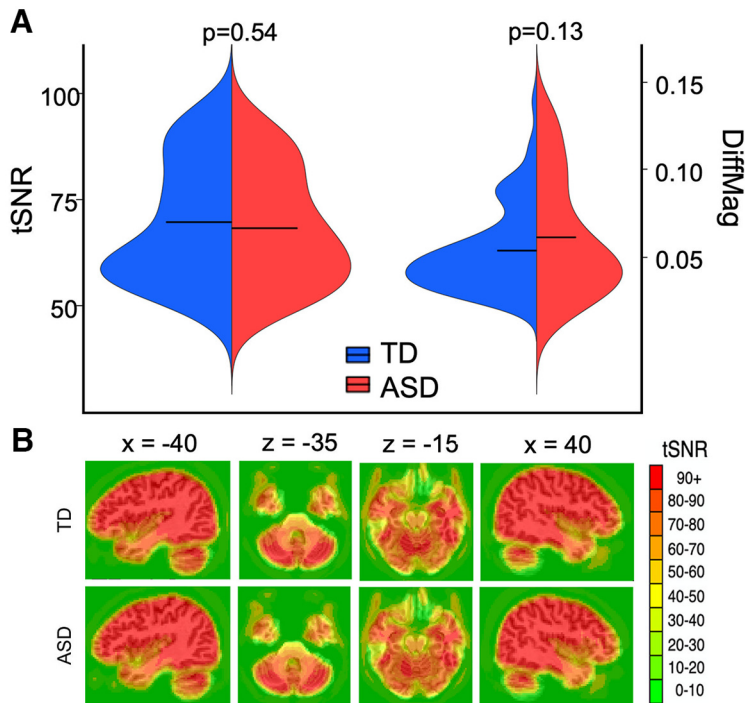
Figure 1. High-quality fMRI data were matched between the groups. ***A***, Both groups had high tSNRs (i.e., time series mean divided by time series SD) and a low level of head motion (as measured using the DiffMag program in AFNI). There were no significant differences between tSNR or DiffMag between the groups. Black horizontal lines in the violin plots represent the mean of each measure in each group. ***B***, Whole-brain maps of the average tSNR across participants from the TD and ASD groups, respectively. The tSNR values were high across the whole brain in both groups.

Experimental design. Homotopic locations in the two hemispheres were identified and aligned using nonlinear volumetric registration with the AFNI 3dQwarp tool (Cox, 1996). Specifically, in each participant, we first flipped the right hemisphere of the anatomic image across the midline so that it was roughly overlapping the left hemisphere. Next, we applied a nonlinear transformation with no blurring to align the right hemisphere with the left. After achieving satisfactory alignment of the right and left hemisphere anatomic images, we applied the same transformation to the resting-state data maps. A consequence of this transformation is that right-hemisphere voxels were tightly aligned to the corresponding left-hemisphere voxels and thus could be projected directly onto the left hemisphere. Therefore, analyses for homotopic voxels in the left and right hemispheres could both be mapped on to the same (left hemisphere) voxels.

Statistical analysis: calculating laterality metrics. The method that we used to calculate the laterality metrics for our analyses has also been used in earlier studies (Liu et al., 2009; Gotts et al., 2013). Specifically, we first aligned the left and right hemispheres in each participant so that each voxel in the left hemisphere was paired with its homotopic voxel in the right hemisphere (Fig. 2A, top). We then correlated the BOLD time series from each voxel with the time series from every other voxel in the same and opposite hemispheres to create within- and across-hemisphere connectivity maps (Fig. 2A, middle). For each voxel, we then averaged the correlation values to all voxels in the within- and across-hemisphere connectivity maps separately and stored the average correlation coefficients (ρ) at the voxel location (Fig. 2A, bottom). Thus, each voxel in the left hemisphere contained two values (LL and LR), and each voxel in the right hemisphere contained two values (RR and RL). The first letter indicates the voxel location, and the second letter indicates the target hemisphere. Importantly, because the unique connectivity pattern between each voxel and each hemisphere is calculated and then averaged separately, the resultant metrics stored within each voxel are independent and therefore result in a unique map for each of the laterality metrics (Fig. 2A, bottom).

Next, we applied Fisher's z′-transform to yield normally distributed values across all voxels. In each voxel, we then calculated two main metrics of laterality—one that measures the tendency for greater within-hemisphere than across-hemisphere communication from the left versus right hemisphere, referred to as Segregation, and another that measures a greater sum of within- and across-hemisphere communication from the left versus right hemisphere, referred to as Integration (Fig. 2B). As previously described by Gotts et al. (2013), the Segregation and Integration equations were designed to test for different types of hemispheric interactions between homotopic left- and right-hemisphere voxels. Using patterns of whole-brain correlations, the Segregation metric is meant to identify areas of the brain where functional connectivity is more restricted to one hemisphere, whereas the Integration metric is meant to identify areas of the brain for which functional connectivity is more bilaterally distributed across cortex and stronger with a location in one hemisphere relative to its homotopic location in the other hemisphere. To measure Segregation, we used an equation that is equivalent to a Seed-X target hemisphere interaction in an ANOVA, (LL - LR)− (RR - RL). Positive results from this equation indicate Left Segregation, and negative values indicate Right Segregation. Whereas a large positive value of one side of this equation (e.g., LL - LR) would indicate a stronger average within- than across-hemisphere correlation from a seed voxel, a large value (positive or negative) of the full Segregation metric tends to indicate that in a given seed or brain region the bias for stronger within-hemisphere interactions is greater in one hemisphere relative to the other. In contrast, the Integration metric is equivalent to a main effect of seed hemisphere in an ANOVA (Liu et al., 2009; Gotts et al., 2013), (LL + LR) − (RR + RL). Positive results from this equation indicate that in a given seed or brain region, bilateral interactions are stronger to a location in the left hemisphere, and negative values indicate stronger bilateral interactions to the homotopic location in the right hemisphere. As with main effects and interactions detected with ANOVA, interpretation of the detailed pattern must be clarified by *post hoc* tests performed on the individual components (LL, LR, RR, RL).

Statistical analysis: identifying functional networks. After calculating the laterality metrics in all voxels, we obtained whole-brain maps of Segregation and Integration for both hemispheres (Fig. 2C). Because these maps contained widespread activation, we then applied a stringent threshold ($p < 10^{-6}$, FDR q < 0.01) to them so we could identify individual regions that could then be clustered into separate functional networks. Next, we extracted the average time series from each region and correlated it with the time series from every voxel in the brain to obtain a whole-brain connectivity pattern for each region. We then correlated the whole-brain patterns of connectivity between the regions and submitted the resultant region times region correlation matrix to *k*-means clustering. Specifically, the square region of interest correlation matrix was iteratively analyzed with *k*-means cluster analysis at progressively larger numbers of clusters (*k*), and each choice of *k* was repeated 100 times for stability.

## Results

Functionally defining a network of interest

Before comparing patterns of laterality between ASD and TD individuals, we first defined functional networks by combining the groups (*N* = 140) and identifying brain regions based on four patterns of laterality, Left segregation, Right segregation, Left integration, and Right integration (Fig. 2C). We found a total of 18 regions across the brain; eight regions identified with the Left-

segregation metric, one with Right segregation, five with Right integration, and four with Left integration ($p < 10^{-6}$, FDR q < 0.01). We submitted the resultant 18 × 18 correlation matrix to k-means clustering and found an optimal trade-off of cluster number and variance explained by k-means clustering at the choice of $k =$ 3 clusters, with ~80% of the variance explained (Fig. 3A). Although the metric used to identify a region did not guarantee that it would be clustered with other regions identified using the same metric, a mostly frontotemporal network comprised seven of the eight regions that were identified using the Left-segregation metric (Fig. 3B, red network)—the inferior frontal gyrus, (dorsal and ventral) medial prefrontal cortex, anterior middle temporal gyrus (MTG)/temporal pole, anterior hippocampus, posterior MTG/superior temporal sulcus, angular gyrus, and posterior cingulate cortex/precuneus. This network also included two regions defined with the right and left Integration metrics, respectively, anterior superior temporal gyrus (aSTG) and lateral anterior temporal pole (Fig. 3D). We used this conglomeration of language and social processing regions (Geschwind, 1972; Binder et al., 1997; Frith and Frith, 2007; Olson et al., 2007; Adolphs, 2009; Mitchell, 2009; Fedorenko et al., 2011) as the primary network of interest (NOI) for further analyses.

Testing four models of reduced laterality in the NOI

We tested the following four models of reduced laterality in the NOI in ASD: a model of increased communication between hemispheres (the Integrated model), a model of no change in the asymmetry of (left) lateralized connectivity between hemispheres (the Left-segregated, or Null, model), a model of decreased laterality in left hemisphere regions accompanied by increased laterality in homotopic regions in the right hemisphere (the Right-segregated model), and a model of strong segregation of the homotopic regions of both hemispheres (the Decoupled-hemispheres model). First, we tested the Integrated model using the Integration metric to ask whether there is more interhemispheric communication in the ASD network compared with the TD group. The Integration metric was not significantly different from zero in either group (both $t_{(138)}$ values < 1, both p values > 0.4, d values < 0.10), and there was not a significant difference between the groups ($t_{(138)} =$ 0.08, $p = 0.94$, $d = 0.01$; Fig. 4A), thus suggesting that reduced laterality in the NOI is not because of an increase in communication across the hemispheres. However, it could be the case that in the ASD group there is an increase in the across-hemisphere component metrics (LR and RL), which measure the strength of communication between the typically left-lateralized network and the left and right hemisphere, respectively, separate from the
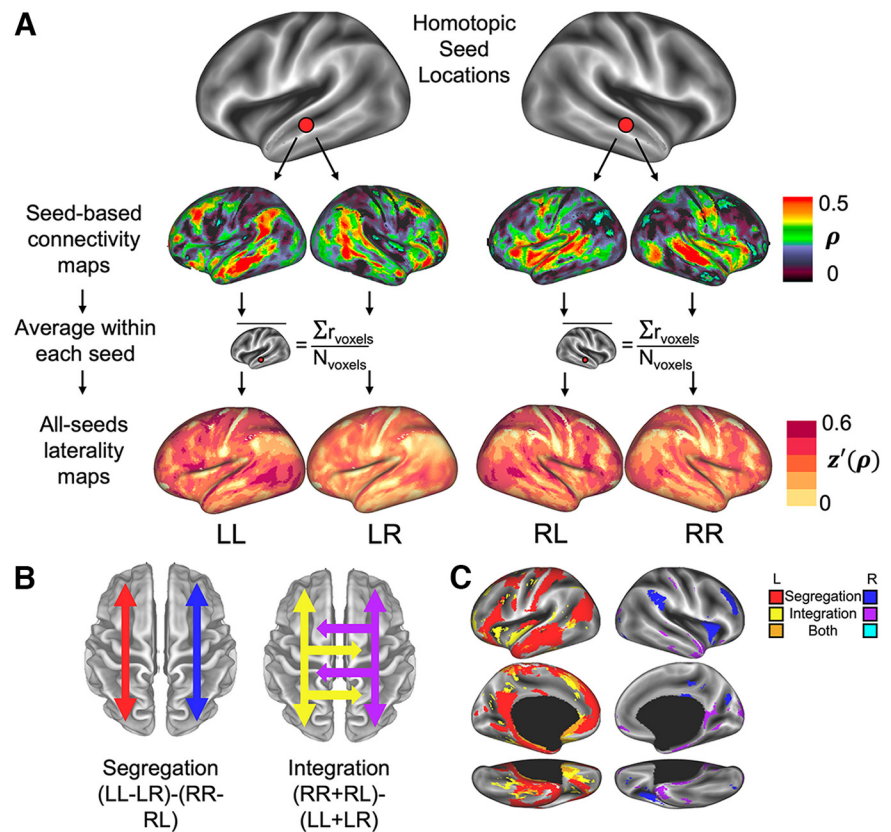

Figure 2. Calculating within- and across-hemisphere connectivity at homotopic locations across the whole brain. *A*, Top, In each participant we aligned the left and right hemispheres so that each voxel in the left hemisphere was paired with its homotopic voxel in the right hemisphere. Middle, Next, we correlated the BOLD time series from each voxel with the time series from every other voxel in the same and opposite hemispheres to create within- and across-hemisphere connectivity maps (data from an individual participant). Bottom, In each voxel, we then averaged the correlation values to all other voxels in the within- and across-hemisphere connectivity maps separately and stored the average correlation coefficients (ρ) at the voxel location (data from an individual participant), so each homotopic pair of voxels contained four values, LL and LR in the left hemisphere and RR and RL in the right hemisphere. We then applied Fisher's z'-transform to yield normally distributed values across all voxels. *B*, Next, we calculated two main metrics of laterality in each voxel, one that measures the degree of within-hemisphere communication from each location in cortex relative to the homotopic location in the other hemisphere, referred to as Segregation, and another that measures across-hemisphere communication, referred to as Integration. *C*, Once we calculated the Segregation and Integration metrics in all voxels in each participant, we then averaged the laterality maps across all participants in both groups ($N = 140$). Finally, we thresholded the maps ($p < 0.001$) to functionally define regions based on their laterality profiles and then used k-means clustering to identify networks of interest for our main analyses.

degree of within-hemisphere or homotopic connectivity. If the across-hemisphere metrics are greater in the ASD than the TD group, it would suggest that left-hemisphere regions in the NOI are communicating more with regions in the right hemisphere. Interestingly, however, we instead found the opposite, that is, decreases in the LR ($t_{(138)} = -1.90$, $p = 0.06$, $d = 0.32$) and RL ($t_{(138)} = -2.42$, $p = 0.02$, $d = 0.41$) metrics in ASD compared with the TD group (Fig. 4C). These results suggest that the typically left-lateralized NOI in ASD is less connected to the right hemisphere, whereas homotopic right regions are less connected with the left hemisphere. [It is worth noting here, that functional connectivity in the NOI was significantly reduced in the ASD compared with TD group (Fig. 4C). This pattern of results is consistent with prior studies that reported reduced connectivity in brain networks that support social communication in ASD relative to the TD group (Kennedy and Courchesne, 2008; Weng et al., 2010; Ebisch et al., 2011; Gotts et al., 2012; Abrams et al., 2013; Alaerts et al., 2014; Jung et al., 2014; Verly et al., 2014; Fishman et al., 2015; Picci et al., 2016; Linke et al., 2018; Jasmin et al., 2019). Critically, this main effect of group does not affect
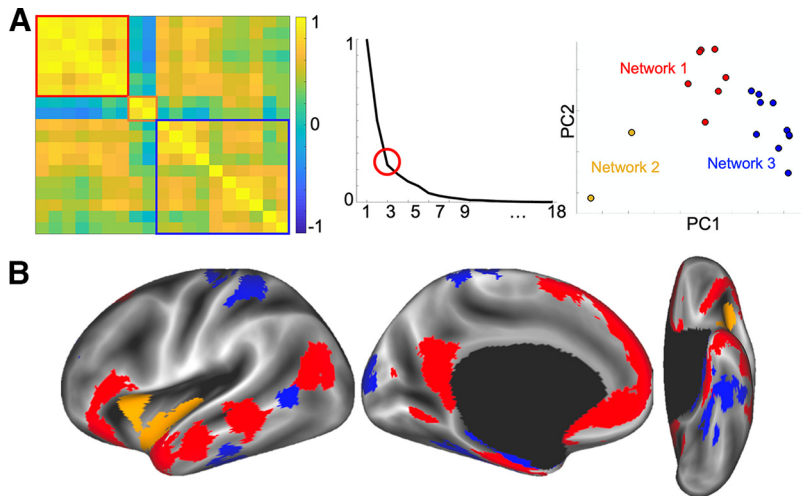
Figure 3. Functionally defined networks of interest. *A*, After we defined 18 regions based on the left and right Segregation and Integration maps, we extracted the time series from each, calculated a whole-brain correlation map from each region, then created an 18 × 18 similarity matrix based on the whole-brain correlation patterns (left). Next, we ran *k*-means clustering on the similarity matrix and found that an optimal solution of *k* = 3 clusters explained ~80% of the variance in the data (middle). Principal components analysis shows the distribution of the 18 regions separated into three clusters in a 2D plot (right). *B*, The three functionally defined networks displayed on an inflated brain. Network 1 (red) is our primary NOI as the regions in it predominantly exhibited strong left Segregation and overlap with previously reported regions related to language and social communication.
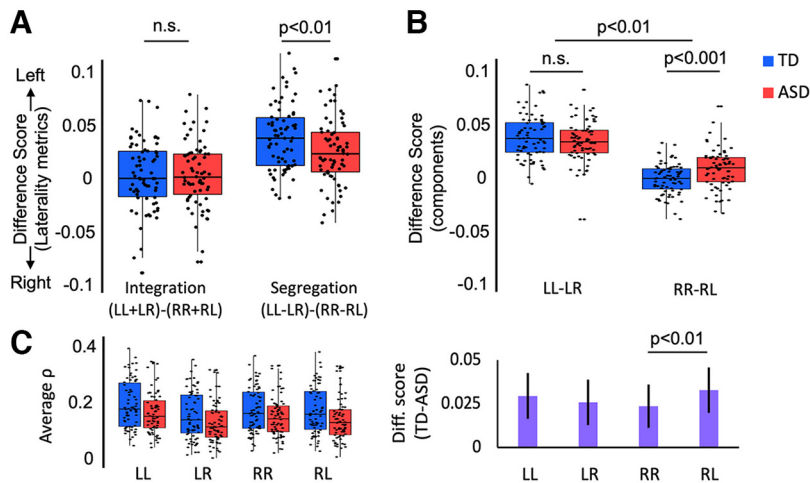
Figure 4. Laterality differences in the NOI. *A*, Integration and Segregation scores displayed as box plots with individual data points overlaid for each group. Positive values indicate leftward Integration/Segregation and negative values indicate rightward Integration/Segregation. The Integration metric did not differ from zero in either group, and there was not a significant difference between groups. In contrast, both groups showed significant left Segregation with a significant decrease in left Segregation in the ASD compared with the TD group. *B*, Comparison of the left- and right-hemisphere components of the Segregation metric separately. Greater values of LL - LR indicate greater within- than across-hemisphere connectivity of regions in the left hemisphere, whereas greater values of RR - RL indicate greater within- than across-hemisphere connectivity of regions in the right hemisphere. There was significantly greater within- than across-hemisphere connectivity in the left hemisphere of both groups but no significant difference between groups. In the right hemisphere, the ASD group showed significantly greater within- than across-hemisphere connectivity, whereas the TD group did not. Furthermore, there was a significant Group times Component interaction. *C*, Left, The correlation coefficient for the component metrics in both groups. Right, The components as across-group difference scores in a bar graph to make the group differences more apparent (Error bars are ±1 SE from the mean.).

our analyses or the interpretation of the results as the laterality metrics rely on within-subject contrasts and are thus effectively normalized across groups.]

Next, we tested the Left-segregated model using the Segregation metric. In the TD group, the NOI exhibited strong leftward segregation (i.e., significantly stronger left laterality compared with

the laterality of homotopic right regions); thus, we can reject the Left-segregated model if there is a significant decrease in this laterality metric in the ASD group. As predicted, a two-sample *t* test revealed a significant decrease in the Left-segregation metric in ASD compared with the TD group ($t_{(138)} = -2.57$, $p = 0.01$, $d = 0.43$), thus suggesting that ASD individuals indeed exhibit atypical left laterality in the NOI (Fig. 4A).

Finally, we tested the Right-segregated and Decoupled-hemispheres models by looking at the components of the Segregation metric separately. As described above, the Segregation metric is a measure of the degree of laterality in voxels of one hemisphere relative to the laterality of homotopic voxels in the other hemisphere. Thus, one side of the equation (LL - LR, or the left-hemisphere component) indicates greater within- than across-hemisphere connectivity in the left hemisphere independent of homotopic regions in the right hemisphere, whereas the other side (RR - RL, or the right-hemisphere component) indicates greater within- than across-hemisphere connectivity at the homotopic points, independent of the left hemisphere. If the Right-segregation model is correct, then we should see a significant decrease in the left-hemisphere component coupled with a significant increase in the right-hemisphere component in the ASD compared with the TD group. In contrast, if the Decoupled-hemispheres model is correct, then we should see no difference in the left-hemisphere component coupled with a significant increase in the right-hemisphere component in the ASD compared with the TD group. A 2 (Group ASD, TD) × 2 (Component Left, Right) two-way ANOVA (Fig. 4B) revealed a significant interaction ($F_{(1,276)} = 9.30$, $p < 0.01$, $\eta P^2 = 0.03$), and planned-comparisons *t* tests showed that there was not a significant difference in the left-hemisphere component between the groups ($t_{(138)} = -1.12$, $p = 0.26$, $d = 0.19$), whereas there was a significant increase in the right-hemisphere component in the ASD compared with the TD group ($t_{(138)} = 3.40$, $p < 0.001$, $d = 0.58$). Although these results support the Decoupled-hemispheres model, it could be the case that the difference in the right-hemisphere component is driven solely by increased connectivity within the right hemisphere (RR) rather than a decrease in connectivity to the left hemisphere (RL) in the ASD group. To ensure that the difference between the groups is because of decreased connectivity between hemispheres in the NOI, we conducted a 2 (Group ASD, TD) × 2 (Seed Lx, Rx) × 2 (Target xR, xL) three-way ANOVA. We found a significant interaction ($F_{(1,138)} = 6.05$, $p < 0.05$, $\eta P^2 = 0.04$) that was driven by a significantly greater decrease in the RL component in the ASD relative to the TD group compared with the difference in RR
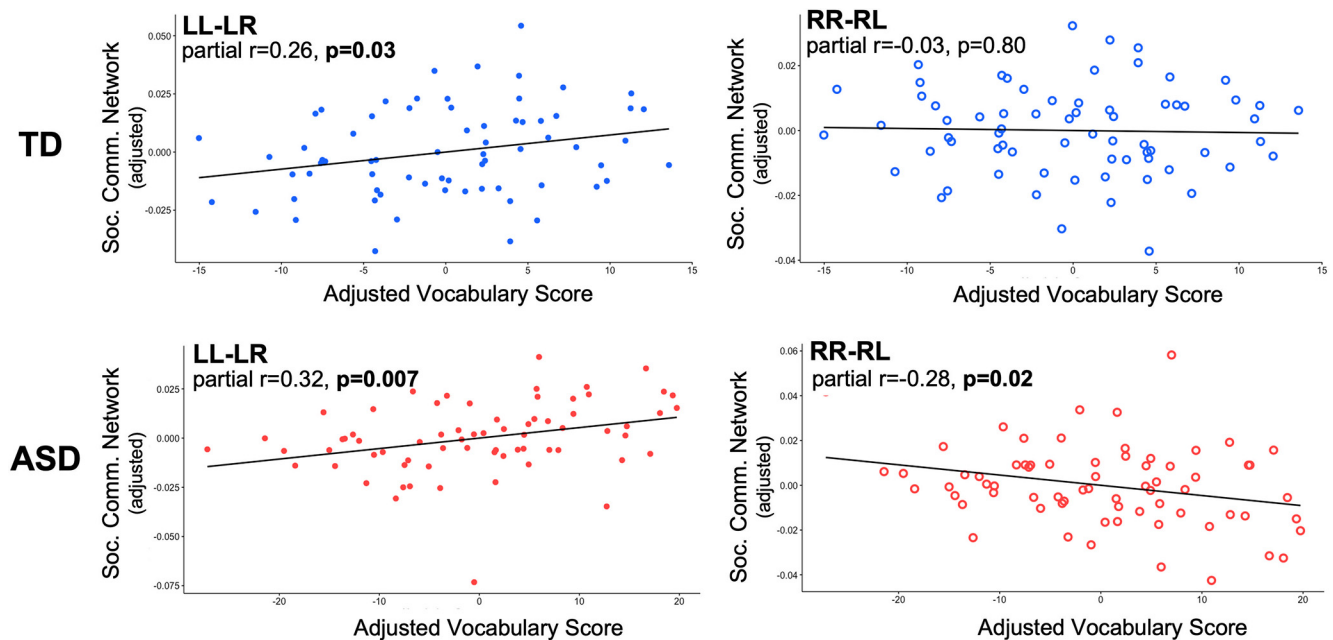
Figure 5. Correlations between the left- and right-hemisphere components and verbal ability. Left, For both TD and ASD groups, the left-hemisphere component in the NOI is positively correlated with verbal ability. Right, In contrast, the right-hemisphere component and verbal ability are not correlated in the TD group, but there is a negative correlation between the two variables in the ASD group. The plotted data are correlations of the residuals of the brain and behavior data after regressing out age, head motion, and Block Design score.

between the groups ($F_{(1,138)} = 11.55$, $p < 0.001$, $\eta P^2 = 0.08$). There was no such interaction between the groups for the LR and LL components ($F_{(1,138)} = 1.27$, $p = 0.26$, $\eta P^2 = 0.01$; Fig. 4C). Together, these results suggest that although the ASD group has an intact left-lateralized network, the homotopic regions in the right hemisphere are communicating more strongly within than across hemisphere relative to the TD group.

Correlations between the left- and right-hemisphere components in the NOI and a measure of verbal ability
Next, we correlated the left- and right-hemisphere component metrics with Vocabulary subtest scores from the WASI (a measure of verbal ability) while covarying the effects of age, Block Design subtest, and head motion. We then compared the correlation coefficients between the groups. We found that verbal ability was positively correlated with the left-hemisphere component in both groups (ASD, $r = 0.38$, $p = 0.002$; TD, $r = 0.26$, $p = 0.03$), whereas verbal ability was negatively correlated with the right-hemisphere component in the ASD ($r = -0.28$, $p = 0.03$) but not the TD group ($r = -0.002$, $p = 0.99$; Fig. 5). Crucially, the negative correlation between verbal ability and the right-hemisphere component metric in the ASD group was significantly different from the same correlation coefficient in the TD group ($z = -1.64$, $p = 0.05$) and significantly different from the within-group correlation coefficient between verbal ability and the left-hemisphere component ($z = -2.46$, $p < 0.01$). Furthermore, neither the left- nor right-hemisphere component was correlated with scores on the Block Design subtest of the WASI (i.e., a measure of visuospatial abilities; both r values < 0.08, both p values > 0.50), the Social Responsiveness Scale (both r values < 0.10, both p values > 0.80), or the Repetitive Behaviors Scale–Revised (both r values < 0.15, both p values > 0.6) while covarying the effects of age, Vocabulary subtest score, and head motion. This pattern of relationships between verbal ability and the left- and right-hemisphere components in ASD further

supports the decoupled-hemispheres model by showing that each hemisphere is covarying independently with the same behavioral measure and suggests that atypically greater within than across hemisphere connectivity in the right hemisphere of the NOI in ASD is a maladaptive trait.

Are these patterns of results specific to the NOI in ASD?
In addition to the typically left-lateralized NOI that was the focus of our analyses, we also identified two other networks using metrics of laterality and k-means clustering (Fig. 3B). One network was composed of regions in the insula and STG that were defined using the Right-segregation and Left-integration metrics. The other network comprised regions in somatosensory, occipital, and dorsal lateral prefrontal cortices, and the parahippocampal gyrus that were defined using the Left and Right integration and Left-segregation metrics. Because a large body of the literature has focused specifically on the typically left-lateralized network (comparable to our NOI) in relation to communication- and language-related deficits in ASD, we predicted that the other two networks would not show the same pattern of atypical laterality. As predicted, there were no significant differences between the groups in any of the laterality metrics (all p values > 0.18). Thus, atypical laterality in the ASD group appears to be specific to the (typically left lateralized) NOI.

Discussion
We tested four models of reduced laterality in a social communication network in ASD individuals using high-quality fMRI data and a resting-state fMRI method of measuring patterns of functional laterality across the brain. We found that the social communication network exhibited the typical pattern of left laterality in ASD when compared with a tightly matched TD control group. However, we also found within the same network a significant increase in within- relative to across-hemisphere connectivity in homotopic regions in the right hemisphere in ASD individuals. In both groups, greater within- than across-hemisphere

connectivity in the left hemisphere was positively correlated with a measure of verbal ability, whereas greater within- than across-hemisphere connectivity in the right hemisphere in ASD, but not TD, was negatively correlated with the same verbal measure. These results suggest that reduced laterality of this network in ASD is because of the two hemispheres functioning more independently than seen in typically developing individuals and that the increase in within- relative to across-hemisphere connectivity in the right hemisphere in this network in ASD is maladaptive. Crucially, these differences in patterns of laterality were not found in two other functional networks and were specifically correlated to a measure of verbal ability.

We designed our experiment to address three shortcomings that are often found in prior studies of differences in patterns of laterality between ASD and TD groups. First, we selected high-quality fMRI data from a relatively large sample of ASD individuals ($N = 70$), as determined by measures of tSNR and head motion (Fig. 1), and a tightly matched control group of TD individuals who were also matched on age and full-score IQ. Therefore, we could be confident that differences between our groups were because of functional changes of interest rather than poor data quality or demographic differences. Second, our method allowed us to define functional networks based on patterns of resting-state correlations and then probe the defined networks with independent measures of laterality, thus freeing us from the need to define a priori networks based on anatomy or coordinates from prior studies. Third, we measured changes to the functional organization of a social communication network in ASD, so we could adjudicate between models of functional laterality that might underlie prior reports of reduced laterality in ASD individuals.

Although several prior studies have used either task-based fMRI or measures of cortical volume to establish that atypical, or reduced, laterality of regions involved in social and communication processes is a stable feature of ASD, it is unclear how the observed changes in laterality are related to the underlying functional organization of the network. In the case of task-based fMRI studies, the evidence for reduced laterality is an imbalance in the relative magnitude of responses between the left- and right-hemisphere regions of the network. For example, several studies have found that during language and communication tasks, the magnitude of responses is significantly greater in the left hemisphere compared with homotopic regions in the right for TD individuals, whereas in ASD individuals the magnitude of responses is either statistically equal between the hemispheres or even stronger in the right hemisphere (Lindell and Hudry, 2013; Herringshaw et al., 2016). Although these results do indeed demonstrate a reduction in the typical left laterality of the network, the functional architecture underlying the reduction remains unknown. Therefore, we used functional connectivity to measure how the organization of the network is changed in ASD. We tested four models of potential changes to the organization of the network that would explain reductions in laterality found using task-based fMRI. Our analyses indicated that although the laterality typically found in left-hemisphere regions is intact in ASD individuals, homotopic regions in the right hemisphere are communicating more strongly within relative to across hemisphere in the ASD compared with TD group. These results suggest that reduced laterality in the functional networks underlying social and communication processes in ASD individuals is because of the left and right hemispheres acting more as independent networks compared with the hemispheric functional dynamics in the TD group. Furthermore, we found that atypically greater

within- than across-hemisphere connectivity in the right-hemisphere regions in ASD individuals is negatively correlated with verbal ability and thus seems to be maladaptive. Intriguingly, these results are consistent with deficits in language and social communication skills related to agenesis of the corpus callosum, a condition that results in reduced communication between hemispheres of the brain (Paul et al., 2003).

In conclusion, we found that previous reports of reduced laterality in regions underlying language and social communication in ASD is a result of the hemispheres behaving more like independent, intrahemispheric networks. We further found that the degree to which right-hemisphere regions are communicating more within than across hemisphere was negatively correlated with verbal ability in ASD. These results offer a detailed account of how patterns of functional laterality shift in a social-communication network in ASD individuals, and, we hope, these results may lead to more precise clinical identification and interventions for social communication deficits in ASD individuals.

References

Abrams DA, Lynch CJ, Cheng KM, Phillips J, Supekar K, Ryali S, Uddin LQ, Menon V (2013) Underconnectivity between voice-selective cortex and reward circuitry in children with autism. Proc Natl Acad Sci U S A 110:12060–12065.

Adolphs R (2009) The social brain: neural basis of social knowledge. Annu Rev Psychol 60:693–716.

Alaerts K, Woolley DG, Steyaert J, Di Martino A, Swinnen SP, Wenderoth N (2014) Underconnectivity of the superior temporal sulcus predicts emotion recognition deficits in autism. Soc Cogn Affect Neurosci 9:1589–1600.

American Psychiatric Association (2013) Diagnostic and statistical manual of mental disorders: DSM-5. Arlington, VA: American Psychiatric Association.

Anderson JS, Lange N, Froehlich A, DuBray MB, Druzgal TJ, Froimowitz MP, Alexander AL, Bigler ED, Lainhart JE (2010) Decreased left posterior insular activity during auditory language in autism. AJNR Am J Neuroradiol 31:131–139.

Binder JR, Frost JA, Hammeke TA, Cox RW, Rao SM, Prieto T (1997) Human brain language areas identified by functional magnetic resonance imaging. J Neurosci 17:353–362.

Birn RM, Smith MA, Jones TB, Bandettini PA (2008) The respiration response function: the temporal dynamics of fMRI signal fluctuations related to changes in respiration. Neuroimage 40:644–654.

Boddaert N, Belin P, Chabane N, Poline J-B, Barthélémy C, Mouren-Simeoni M-C, Brunelle F, Samson Y, Zilbovicius M (2003) Perception of complex sounds: abnormal pattern of cortical activation in autism. Am J Psychiatry 160:2057–2060.

Boucher J (2003) Language development in autism. Int Congr Ser 1254:247–253.

Boucher J (2012) Research review: structural language in autistic spectrum disorder—characteristics and causes. J Child Psychol Psychiatry 53:219–233.

Constantino JN, Davis SA, Todd RD, Schindler MK, Gross MM, Brophy SL, Metzger LM, Shoushtari CS, Splinter R, Reich W (2003) Validation of a brief quantitative measure of autistic traits: comparison of the social responsiveness scale with the autism diagnostic interview-revised. J Autism Dev Disord 33:427–433.

Corbetta M, Shulman GL (2011) Spatial neglect and attention networks. Annu Rev Neurosci 34:569–599.

Cox RW (1996) AFNI: software for analysis and visualization of functional magnetic resonance neuroimages. Comput Biomed Res 29:162–173.

Ebisch SJH, Gallese V, Willems RM, Mantini D, Groen WB, Romani GL, Buitelaar JK, Bekkering H (2011) Altered intrinsic functional connectivity of anterior and posterior insula regions in high-functioning participants with autism spectrum disorder. Hum Brain Mapp 32:1013–1028.

Eyler LT, Pierce K, Courchesne E (2012) A failure of left temporal cortex to specialize for language is an early emerging and fundamental property of autism. Brain 135:949–960.

Fedorenko E, Behr MK, Kanwisher N (2011) Functional specificity for high-level linguistic processing in the human brain. Proc Natl Acad Sci U S A 108:16428–16433.

Fischl B, Salat DH, Busa E, Albert M, Dieterich M, Haselgrove C, Van Der Kouwe A, Killiany R, Kennedy D, Klaveness S, Montillo A, Makris N, Rosen B, Dale AM (2002) Whole brain segmentation: automated labeling of neuroanatomical structures in the human brain. Neuron 33:341–355.

Fishman I, Datko M, Cabrera Y, Carper RA, Müller R-A (2015) Reduced integration and differentiation of the imitation network in autism: a combined functional connectivity magnetic resonance imaging and diffusion-weighted imaging study. Ann Neurol 78:958–969.

Frith CD, Frith U (2007) Social cognition in humans. Curr Biol 17:R724–R732.

Geschwind N (1972) Language and the brain. Sci Am 226:76–83.

Glover GH, Li T-Q, Ress D (2000) Image-based method for retrospective correction of physiological motion effects in fMRI: RETROICOR. Magn Reson Med 44:162–167.

Goldstein G, Minshew NJ, Siegel DJ (1994) Age differences in academic achievement in high-functioning autistic individuals. J Clin Exp Neuropsychol 16:671–680.

Gotts SJ, Simmons WK, Milbury LA, Wallace GL, Cox RW, Martin A (2012) Fractionation of social brain circuits in autism spectrum disorders. Brain 135:2711–2725.

Gotts SJ, Jo HJ, Wallace GL, Saad ZS, Cox RW, Martin A (2013) Two distinct forms of functional lateralization in the human brain. Proc Natl Acad Sci U S A 110:E343–E3444.

Harris GJ, Chabris CF, Clark J, Urban T, Aharon I, Steele S, McGrath L, Condouris K, Tager-Flusberg H (2006) Brain activation during semantic processing in autism spectrum disorders via functional magnetic resonance imaging. Brain Cogn 61:54–68.

Herbert MR, Harris GJ, Adrien KT, Ziegler DA, Makris N, Kennedy DN, Lange NT, Chabris CF, Bakardjiev A, Hodgson J, Takeoka M, Tager-Flusberg H, Caviness VS (2002) Abnormal asymmetry in language association cortex in autism. Ann Neurol 52:588–596.

Herringshaw AJ, Ammons CJ, DeRamus TP, Kana RK (2016) Hemispheric differences in language processing in autism spectrum disorders: a meta-analysis of neuroimaging studies. Autism Res 9:1046–1057.

Jasmin K, Gotts SJ, Xu Y, Liu S, Riddell CD, Ingeholm JE, Kenworthy L, Wallace GL, Braun AR, Martin A (2019) Overt social interaction and resting state in young adult males with autism: core and contextual neural features. Brain 142:808–822.

Jo HJ, Saad ZS, Simmons WK, Milbury LA, Cox RW (2010) Mapping sources of correlation in resting state FMRI, with artifact detection and removal. Neuroimage 52:571–582.

Jouravlev O, Kell AJE, Mineroff Z, Haskins AJ, Ayyash D, Kanwisher N, Fedorenko E (2020) Reduced language lateralization in autism and the broader autism phenotype as assessed with robust individual-subjects analyses. Autism Res 13:1746–1761.

Jung M, Kosaka H, Saito DN, Ishitobi M, Morita T, Inohara K, Asano M, Arai S, Munesue T, Tomoda A, Wada Y, Sadato N, Okazawa H, Iidaka T (2014) Default mode network in young male adults with autism spectrum disorder: relationship with autism spectrum traits. Mol Autism 5:35.

Kennedy DP, Courchesne E (2008) Functional abnormalities of the default network during self- and other-reflection in autism. Soc Cogn Affect Neurosci 3:177–190.

Kenworthy L, Wallace GL, Birn R, Milleville SC, Case LK, Bandettini PA, Martin A (2013) Aberrant neural mediation of verbal fluency in autism spectrum disorders. Brain Cogn 83:218–226.

Kleinhans NM, Müller R-A, Cohen DN, Courchesne E (2008) Atypical functional lateralization of language in autism spectrum disorders. Brain Res 1221:115–125.

Knaus TA, Silver AM, Lindgren KA, Hadjikhani N, Tager-Flusberg H (2008) fMRI activation during a language task in adolescents with ASD. J Int Neuropsychol Soc 14:967–979.

Knaus TA, Silver AM, Kennedy M, Lindgren KA, Dominick KC, Siegel J, Tager-Flusberg H (2010) Language laterality in autism spectrum disorder and typical controls: a functional, volumetric, and diffusion tensor MRI study. Brain Lang 112:113–120.

Lackner JR, Teuber H-L (1973) Alterations in auditory fusion thresholds after cerebral injury in man. Neuropsychologia 11:409–415.

Lam KSL, Aman MG (2007) The Repetitive Behavior Scale–Revised: independent validation in individuals with autism spectrum disorders. J Autism Dev Disord 37:855–866.

Lindell AK, Hudry K (2013) Atypicalities in cortical structure, handedness, and functional lateralization for language in autism spectrum disorders. Neuropsychol Rev 23:257–270.

Linke AC, Jao Keehn RJ, Pueschel EB, Fishman I, Müller R-A (2018) Children with ASD show links between aberrant sound processing, social symptoms, and atypical auditory interhemispheric and thalamocortical functional connectivity. Dev Cogn Neurosci 29:117–126.

Liu H, Stufflebeam SM, Sepulcre J, Hedden T, Buckner RL (2009) Evidence from intrinsic activity that asymmetry of the human brain is controlled by multiple factors. Proc Natl Acad Sci U S A 106:20499–20503.

Mitchell JP (2009) Social psychology as a natural kind. Trends Cogn Sci 13:246–251.

Olson IR, Plotzker A, Ezzyat Y (2007) The enigmatic temporal pole: a review of findings on social and emotional processing. Brain 130:1718–1731.

Paul LK, Van Lancker-Sidtis D, Schieffer B, Dietrich R, Brown WS (2003) Communicative deficits in agenesis of the corpus callosum: nonliteral language and affective prosody. Brain Lang 85:313–324.

Persichetti AS, Denning JM, Gotts SJ, Martin A (2021) A data-driven functional mapping of the anterior temporal lobes. J Neurosci 41:6038–6049.

Picci G, Gotts SJ, Scherf KS (2016) A theoretical rut: revisiting and critically evaluating the generalized under/over-connectivity hypothesis of autism. Dev Sci 19:524–549.

Poeppel D (2003) The analysis of speech in different temporal integration windows: cerebral lateralization as "asymmetric sampling in time". Speech Commun 41:245–255.

Power JD, Barnes KA, Snyder AZ, Schlaggar BL, Petersen SE (2012) Spurious but systematic correlations in functional connectivity MRI networks arise from subject motion. Neuroimage 59:2142–2154.

Power JD, Lynch CJ, Gilmore AW, Spreng SJ, Martin A (2019) Reply to Spreng et al.: Multiecho fMRI denoising does not remove global motion-associated respiratory signals. Proc Natl Acad Sci U S A 116:19243–19244.

Ramot M, Kimmich S, Gonzalez-Castillo J, Roopchansingh V, Popal H, White E, Gotts SJ, Martin A (2017) Direct modulation of aberrant brain network connectivity through real-time NeuroFeedback. Elife 6:e28974.

Rapin I, Dunn M (2003) Update on the language disorders of individuals on the autistic spectrum. Brain Dev 25:166–172.

Redcay E, Courchesne E (2008) Deviant functional magnetic resonance imaging patterns of brain activity to speech in 2–3-year-old children with autism spectrum disorder. Biol Psychiatry 64:589–598.

Semmes J (1968) Hemispheric specialization: a possible clue to mechanism. Neuropsychologia 6:11–26.

Takeuchi M, Harada M, Matsuzaki K, Nishitani H, Mori K (2004) Difference of signal change by a language task on autistic patients using functional MRI. J Med Invest 51:59–62.

Tesink CMJY, Buitelaar JK, Petersson KM, van der Gaag RJ, Kan CC, Tendolkar I, Hagoort P (2009) Neural correlates of pragmatic language comprehension in autism spectrum disorders. Brain 132:1941–1952.

Verly M, Verhoeven J, Zink I, Mantini D, Peeters R, Deprez S, Emsell L, Boets B, Noens I, Steyaert J, Lagae L, De Cock P, Rommel N, Sunaert S (2014) Altered functional connectivity of the language network in ASD: role of classical language areas and cerebellum. Neuroimage Clin 4:374–382.

Wang AT, Lee SS, Sigman M, Dapretto M (2006) Neural basis of irony comprehension in children with autism: the role of prosody and context. Brain 129:932–943.

Warrington EK, James M, Maciejewski C (1986) The WAIS as a lateralizing and localizing diagnostic instrument: a study of 656 patients with unilateral cerebral lesions. Neuropsychologia 24:223–239.

Wechsler D (1999) Wechsler abbreviated scale of intelligence. San Antonio: Psychological.

Weng S-J, Wiggins JL, Peltier SJ, Carrasco M, Risi S, Lord C, Monk CS (2010) Alterations of resting state functional connectivity in the default network in adolescents with autism spectrum disorders. Brain Res 1313:202–214.